Journal of Catalysis **194,** 318–329 (2000)
doi:10.1006/jcat.2000.2925, available online at http://www.idealibrary.com on IDEAL®

Activity of Co Ion Sites in ZSM-5, Ferrierite, and Mordenite in Selective Catalytic Reduction of NO with Methane

Dalibor Kaucký, Alena Vondrová, Jiří Dědeček, and Blanka Wichterlová[1]

J. Heyrovský Institute of Physical Chemistry, Academy of Sciences of the Czech Republic, Dolejškova 3, CZ-182 23 Prague 8, Czech Republic

Received February 7, 2000; revised May 8, 2000; accepted May 12, 2000

Selective catalytic reduction of NO with methane (CH_4-SCR) in an excess of oxygen was investigated over CoH–, CoNa–, CoNaK–, CoBa–, and Co_xO_y–Co-zeolites of ZSM-5, ferrierite, and mordenite structures. The exchanged Co ions have been shown to exhibit activity in CH_4-SCR of NO, while protons or oxide-like Co species in Co–zeolites contribute to the CH_4-SCR activity mostly by enhancement of the oxidation of NO to NO_2. The sequence of Co–zeolites activity in CH_4-SCR of NO (per zeolite weight) was Co–ZSM-5 $\cong$ Co–ferrierite $\gg$ Co–mordenite for the highest Co loadings at Si/Al of 12, 8.4, and 9.2, but for the average Co ion site in the zeolite (in terms of turnover frequency, TOF, values) it was Co–ZSM-5 $>$ Co–ferrierite $\gg$ Co–mordenite. From a comparison of the dependence of TOF values for NO conversion to N_2 per Co ion and of the relative concentrations of the exchanged α-, β-, and γ-type Co ions (determined from quantitative analysis of the characteristic Co(II) Vis spectra) on the total Co concentration, the most active Co sites were estimated. The α-type Co ions, bound to framework oxygens of the wall of the main channel of mordenite and ferrierite, are the most active among the Co ions in these zeolites. On the other hand, in ZSM-5 the β-type Co ions, coordinated to the deformed six-membered ring at the intersection of straight and sinusoidal channels possess the highest activity. The main factors contributing to the individual Co ions' activity are suggested to be cation location in the inner zeolite volume, coordination to the framework, and distances between the Co ions.

Key Words: **NO; SCR of NO; Co zeolites; Co ions; Co–ZSM-5; Co–ferrierite; Co–mordenite.**

INTRODUCTION

SCR of NO_x by low paraffins, including methane, in an excess of oxygen has appeared to be a promising method for abatement of NO_x from flue exhaust gases, as produced by combustion processes (1–3). Ion-exchanged Co–ZSM-5, Co–ferrierite (4–6), and Ga– and In–ZSM-5 zeolites (7–9) containing low amounts of aluminium (Si/Al molar ratio $>$ 8) and pentasil rings in their frameworks have been shown to exhibit high activity and selectivity to nitrogen in CH_4-SCR of NO in an acceptable temperature range, 350–500°C. Such activity, stable in the time on stream, was not reported either with these cations implanted in zeolites with frameworks containing high concentrations of aluminium (Si/Al, ca. 2.5) or for cobalt oxides dispersed on inorganic amorphous carriers. It has also been found that the CH_4-SCR activity of Co–ferrierites and Co–ZSM-5 is not linearly proportional to the concentration of the Co ions (4, 5). This indicated the presence of Co ions with different activities. All these findings point out that siting and coordination of the Co ions at different cationic sites of zeolites might be an important factor affecting their catalytic activity. However, siting and coordination of the Co ions to framework oxygens and of transition metal ions generally, in pentasil ring zeolites have not been known and have not been accessible from the standard XRD analysis (cf. Ref. (10)).

Our approach to estimation of the cationic sites of Co ions in mordenite, ferrierite, and ZSM-5 zeolites was based on the determination of characteristic Vis spectra of the Co(II) ions in these zeolites (11–13) and local framework structures known from XRD (10). Three types of cationic sites for the Co(II) ions (denoted as α, β, and γ) were suggested in mordenite, ferrierite, and ZSM-5 structures (see the Discussion, Figs. 12 and 13). The distribution of the individual Co ion types in these zeolites was determined by quantitative analysis of the Co ion Vis spectra (11–13). Investigations of the perturbation of the local framework T–O–T bonds hosting the α-, β-, and γ-type Co ion sites by monitoring antisymmetric T–O–T IR vibrations in a skeletal window indicated the sequence in the strength of bonding of these Co ions to framework oxygens at the cationic sites (3, 14, 15) to be Co-α $<$ Co-β $<$ Co-γ. Details on the structure and location of the individual Co ions are given in the preceding paper (16).

Different types of bonding of the α-, β-, and γ-type Co ions in pentasil ring zeolites have been shown to be reflected also in their different reactivities with respect to NO bonding (16) and activity in CH_4-SCR of NO (17), as demonstrated for Co–ferrierites. The most open and weakly bound α-type Co ions in ferrierite were the most active and exhibited a high tendency to the formation of dinitrosyls compared to the other types of Co ions.

[1] To whom correspondence should be addressed. E-mail: wichterl@jh-inst.cas.cz.

0021-9517/00 $35.00

CH_4-SCR of NO with methane is a complex reaction, where an excess of oxygen in the reaction mixture is a necessary condition for the catalytic reaction performance (4, 5, 18, 19). This observation and investigations of the CH_4-SCR with NO_2 led to the conclusion that the oxidation of NO to NO_2 represents the first step of the process, followed by the reduction of NO_x by methane, which is at the same time oxidized to CO_2 and/or CO (4, 5, 17, 18). While oxygen is necessary to produce NO_2, on the other hand, it competes with NO_x for methane oxidation. Single exchanged Co ions in ZSM-5 and ferrierite were suggested to be responsible for SCR of NO_x by methane, while oxidic Co_xO_y species were considered to provide activity for oxidation of NO to NO_2 (20).

This paper analyzes and compares the activity and selectivity of Co ions exchanged in zeolites with MFI, FER, and MOR structures in CH_4-SCR of NO. An attempt is made to determine and understand the activity of the Co ions at different cationic sites of these zeolites from the viewpoint of their coordination and bonding to framework oxygens as well as location in the zeolite structures. To evaluate the CH_4-SCR activity of the individual Co ions at different sites, the contribution to this reaction of the protonic sites and "supported" cobalt oxide-like species, in some cases present with the Co ions in zeolites, has also been investigated.

EXPERIMENTAL

Catalyst Preparation

NaK–FER of chemical composition (in wt%) 85.4 SiO_2, 8.62 Al_2O_3, 2.65 Na_2O, 3.24 K_2O, and 0.14 H_2O (Si/Al = 8.4), NH_4–MFI zeolite (both TOSOH Corp., Japan) of composition (in wt%) 92.6 SiO_2, 6.29 Al_2O_3, and 1.12 H_2O (Si/Al = 12.5), and Na–MFI zeolite (kindly provided by the Institute of Oil and Hydrocarbon Gases, Slovakia) of composition (in wt%) 91.2 SiO_2, 5.49 Al_2O_3, and 3.24 Na_2O (Si/Al = 14.1) were used as parent zeolites. NH_4–FER was prepared from NaK–FER by ion exchange at room temperature (RT) with 1.0 M NH_4NO_3; see Ref. (16). The XRD proved the existence of a pure, crystalline zeolite phase. Transmission electron micrographs showed small crystals (average size 1–2 μm) of parent zeolites.

$CoNH_4$–FER (0.40–3.62 wt% Co), CoNaK–FER (0.12–2.60 wt% Co) and $CoNH_4$–MFI (0.94–3.83 wt% Co), CoNa–MFI (0.50–2.29 wt% Co) were prepared by Co ion exchange of the corresponding parent zeolites with $Co(NO_3)_2$ or $Co(acetate)_2$ solutions at RT or 70°C; the latter temperature was used to obtain highly loaded samples. The pH of the solution with a zeolite was kept at a constant value of 5.5 during ion exchange by dosing with 0.01 M HNO_3. Finally, the zeolites were thoroughly washed with distilled water and dried in air. Detailed parameters of the Co ion exchange for Co–FER and Co–MFI zeolites are given in Refs. (12) and (13), respectively.

CoH–MOR (3.55 wt% Co) was prepared from H–MOR of chemical composition (in wt%) 89.4 SiO_2, 8.98 Al_2O_3, and 1.58 H_2O (Si/Al = 8.5) by ion exchange with 0.1 M $Co(NO_3)_2$ at RT, followed by calcination in air at 500°C and repeated Co ion exchange. CoBa–MOR (0.87 wt% Co) was prepared by ion exchange of H–MOR with 0.1 M $Ba(NO_3)_2$, calcination in oxygen at 500°C, and ion exchange with 0.1 M $Co(NO_3)_2$. KCo–MOR (0.50 wt% Co) was prepared from H–MOR by ion exchange with 0.1 M $Co(NO_3)_2$ at RT, calcination in oxygen at 500°C, and ion exchange with 0.05 M KNO_3. Details of the preparation of Co–MOR zeolites are given in Ref. (11).

Cobalt oxide-like species in Co–FER were prepared from the ion-exchanged CoNaK–FER/0.12 by dosing 0.01 M NaOH into a suspension of CoNaK–FER in water to keep the pH at 10. $Co_xO_y(OH)_z$ species were expected to be formed and converted by calcination at a temperature of 500°C into undefined oxide-like Co_xO_y species; the zeolite was denoted as Co_xO_y–Co–FER. Chemical analysis of Co–zeolites, after their dissolution, was done by atomic absorption spectrometry and is given in Table 1. The chemical composition of a zeolite, denoted as, e.g., $CoNH_4$–MFI/0.5, means cobalt ions exchanged into the NH_4 form of a zeolite, Co/Al molar ratio of 0.5.

TABLE 1

Chemical Composition of Co–Zeolites on Dry Bases

Zeolite	Co wt%	Co/Al	Si/Al
$CoNH_4$–FER	0.40	0.05	8.4
$CoNH_4$–FER	0.63	0.07	8.4
$CoNH_4$–FER	2.08	0.23	8.4
$CoNH_4$–FER	2.16	0.25	8.4
$CoNH_4$–FER	3.62	0.42	8.4
CoNaK–FER	0.12	0.01	8.4
CoNaK–FER	0.27	0.03	8.4
CoNaK–FER	0.52	0.06	8.4
CoNaK–FER	0.64	0.07	8.4
CoNaK–FER	1.01	0.12	8.4
CoNaK–FER	1.52	0.18	8.4
CoNaK–FER	2.47	0.28	8.4
CoNaK–FER	2.60	0.31	8.4
$CoNH_4$–MFI	0.94	0.13	12.5
$CoNH_4$–MFI	1.55	0.23	12.5
$CoNH_4$–MFI	2.87	0.42	12.5
$CoNH_4$–MFI	3.14	0.46	12.5
$CoNH_4$–MFI	3.83	0.55	12.5
CoNa–MFI	0.50	0.09	14.1
CoNa–MFI	0.54	0.10	14.1
CoNa–MFI	0.83	0.15	14.1
CoNa–MFI	1.21	0.22	14.1
CoNa–MFI	2.29	0.41	14.1
CoK–MOR	0.50	0.06	8.5
CoBa–MOR	0.87	0.10	8.5
CoH–MOR	3.55	0.35	8.5

Catalyst Characterization

Diffuse reflectance Vis spectra of Co-zeolites (dehydrated at 480°C) were collected by a Perkin–Elmer Lambda 19 UV–Vis–NIR spectrometer equipped with a diffuse reflectance attachment with an integrating sphere coated by $BaSO_4$. The parent zeolite, treated under the same conditions as the Co–zeolites, served as a reference. The Vis spectra of Co–MOR, Co–FER, and Co–MFI are given in Refs. (11), (12), and (13), respectively. The relative concentrations of the α-, β-, and γ-type Co(II) ions in these zeolites were determined from the integral intensities of the corresponding Vis spectral components and absorption coefficients of the individual Co ions in mordenite, ferrierite, and ZSM-5 (for details on the spectra recording and quantitative analysis, see Refs. (11–13).

IR spectra of Co-zeolites (dehydrated at 480°C) in the region of OH groups, 4000–3000 cm^{-1}, were monitored to determine the concentration of protonic sites. The spectra were recorded on thin transparent plates (thickness ca. 7 mg cm^{-2}) placed in a heatable cell connected to a vacuum system at ambient temperature on a Nicolet Magna-IR system 550 FT-IR spectrometer, with a MCT-B detector cooled with liquid nitrogen. From the integral intensities of the band of the bridging OH groups at 3610 (MFI and MOR) and 3604 cm^{-1} (FER) and by using the extinction coefficient given in Ref. (21), the concentration of the protonic sites relative to the total number of available exchangeable sites was determined.

Catalytic Experiments

SCR of NO with CH_4 on Co-zeolites was carried out in a quartz through-flow microreactor, typically with 400 mg of the catalyst. The reactant stream, containing 900 ppm NO, 1200 ppm CH_4, 25,000 ppm O_2, and the rest helium, was kept constant at a total flow of 100 ml/min. The corresponding GHSV was 7500 h^{-1}, assuming a specific catalyst density of 0.5 g cm^{-3}. The catalyst was pretreated in a helium stream at 450°C for 1 h. Then, the reactor was cooled down to a temperature of 200–300°C and contacted with a flow of the reaction mixture. A catalytic test was then carried out typically for 2 h; NO conversion reached a constant value usually within 30 min. After the catalytic test, the temperature of the reactor was increased (at a rate of 5 K/min) up to the next selected temperature with the catalyst under the stream of reactants. In a separate experiment methane was oxidized by gaseous oxygen at a similar feed composition, i.e., 1000 ppm CH_4, 25,000 ppm O_2, and the rest helium at a total flow rate of 100 ml/min.

The product composition was analyzed as follows. Concentrations of NO and NO_2 in the inlet and outlet of the reactor were monitored by a NO/NO_x luminescence analyzer (VAMET-CZ). Concentrations of CH_4, N_2, CO, and N_2O were determined by a gas chromatograph Hewlett Packard 5890 II, equipped with a fused silica column (molecular sieve, 5 Å; length, 30 m; i.d., 0.53 mm; inner coating, 25 μm). Other products, HCN, organic oxygenates, or isocyanate-like substances, were checked for selected experiments by an off-line gas chromatographic analyzer with a mass selective detector.

The conversion values were defined as

$$x_i\ (\%) = \frac{c_i^0 - c_i}{c_i^0} \times 100 \qquad [1]$$

for total conversion of NO and CH_4; i.e., x_{NO} and x_{CH_4}, where c_i^0 is the concentration of the reactant (NO or CH_4) before and c_i is the concentration of the reactant after the reaction.

Conversion of NO to N_2 and NO_2 or CH_4 to CO or CO_2 was given by the equation

$$x_j\ (\%) = \frac{c_j}{c_i^0} \times 100, \qquad [2]$$

where c_j means the concentration of NO_2, $2xN_2$ or CO_2, CO in the reactor outlet.

The turnover frequency (TOF) was defined as molecules of NO converted to N_2 per second and Co atom present in a zeolite.

RESULTS

Depending on the reaction conditions, the CH_4-SCR of NO over H–, CoH–, and CoNa–zeolites resulted in the formation of N_2, NO_2, CO, and CO_2. No N_2O, organic oxygenates, or nitrogen-containing products were detected in the gaseous phase.

Conversion of NO in CH_4-SCR over H–Zeolites

Parent H–MFI, H–FER, and H–MOR exhibited, with increasing temperature, increasing conversion of NO to nitrogen in CH_4-SCR (see Figs. 1 and 2). The activity of H–MFI was higher compared to those of H–MOR and H–FER, but much lower in comparison with the activity of CoH–MFI zeolites. In the temperature range of 200–400°C, NO was preferably oxidized to NO_2, but due to the thermodynamic equilibrium, the concentration of NO_2 was suppressed above 400°C. Methane was not completely oxidized to carbon dioxide, and roughly half of it was converted to carbon monoxide. Na forms of all the zeolites were completely inactive.

Conversion of NO in CH_4-SCR over Ion-Exchanged Co-Zeolites

Figure 3 shows the dependence of conversion of NO to NO_2 and N_2 and conversion of CH_4 to CO_2 on CoH–MFI, typical for all the investigated Co-zeolites. With increasing temperature up to 300°C, the converted NO was preferably

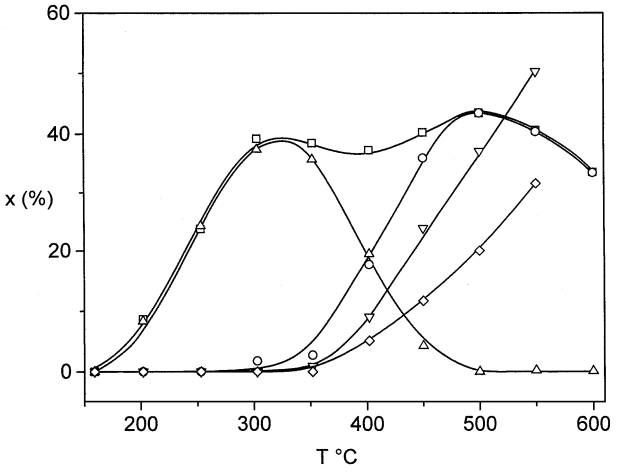

FIG. 1. Dependence of conversion of (—❐—) NO, (—△—) NO to NO_2, (—○—) NO to N_2, (—▽—) CH_4, and (—◇—) CH_4 to CO on temperature in SCR of NO with CH_4 over H–MFI.

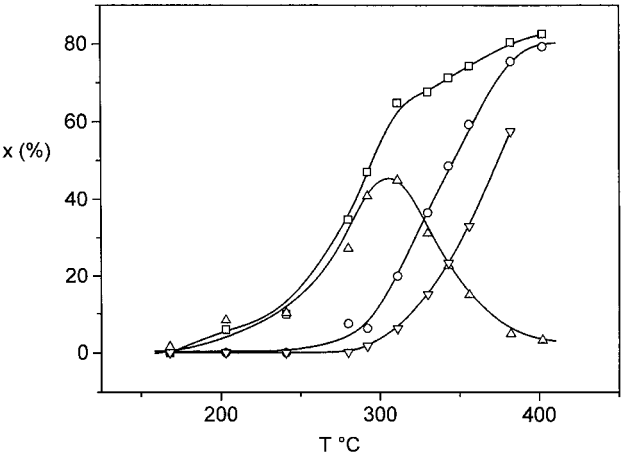

FIG. 3. Dependence of conversion of (—❐—) NO and (—▽—) CH_4 and of NO (—○—) to N_2 and to (—△—) NO_2 in SCR of NO with CH_4 on temperature over CoH–MFI/0.55.

oxidized to NO_2. At this temperature SCR of NO to nitrogen started to take place, being accompanied by the oxidation of CH_4 to CO_2; only for Co–MOR was carbon monoxide, as well as CO_2, observed in the products. Maximum conversion of NO to N_2 was attained at ca. 400°C, when conversion of NO to NO_2 approached zero. Above this temperature, the conversion of NO decreased, while conversion of methane was continuously increased, because of its oxidation by gaseous oxygen. If the reaction temperature was again decreased below that exhibiting maximum conversion, the original conversion values were restored, indicating that the state of cobalt in the zeolite was preserved. This effect was observed for all the Co-zeolites.

With increasing concentration of the Co ions in CoH– and CoNa–ZSM-5 (Fig. 4) and in CoH– and CoNaK–ferrierite (Fig. 5), conversion of NO to nitrogen increased and the maxima of the conversion vs temperature profiles were shifted to lower temperatures. The temperature profiles for zeolites differing in cobalt concentration indicate that

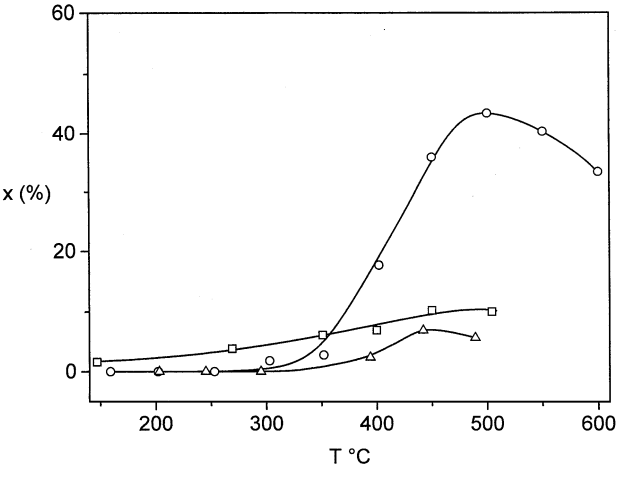

FIG. 2. Dependence of conversion of NO to N_2 on temperature in SCR of NO with CH_4 over (—○—) H–MFI, (—❐—) H–FER, and (—△—) H–MOR.

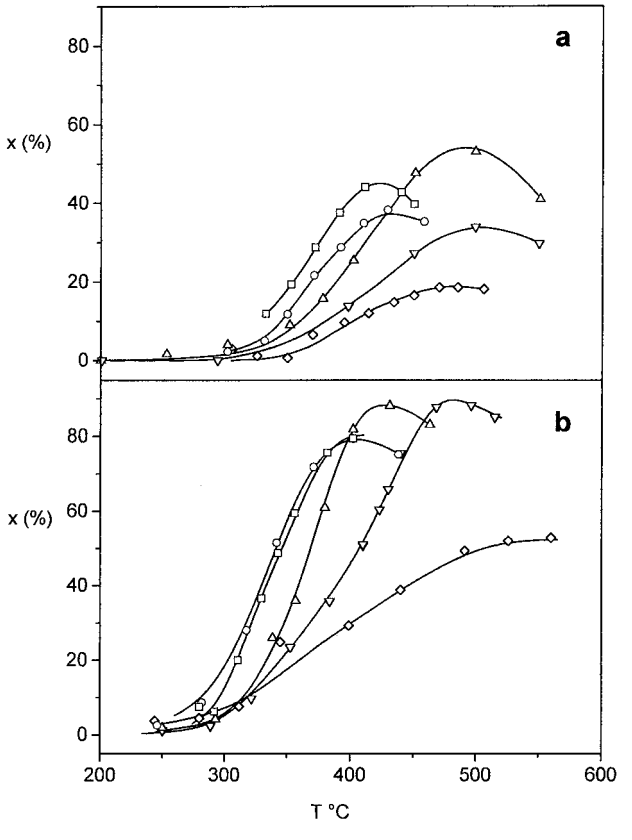

FIG. 4. Dependence of conversion of NO to N_2 in SCR of NO with CH_4 on temperature and Co/Al loading for (a) CoNa–MFI (—❐—) 0.41, (—○—) 0.22, (—△—) 0.15, (—▽—) 0.10, (—◇—) 0.09; (b) CoH–MFI (—❐—) 0.55, (—○—) 0.46, (—△—) 0.42, (—▽—) 0.23, (—◇—) 0.13.

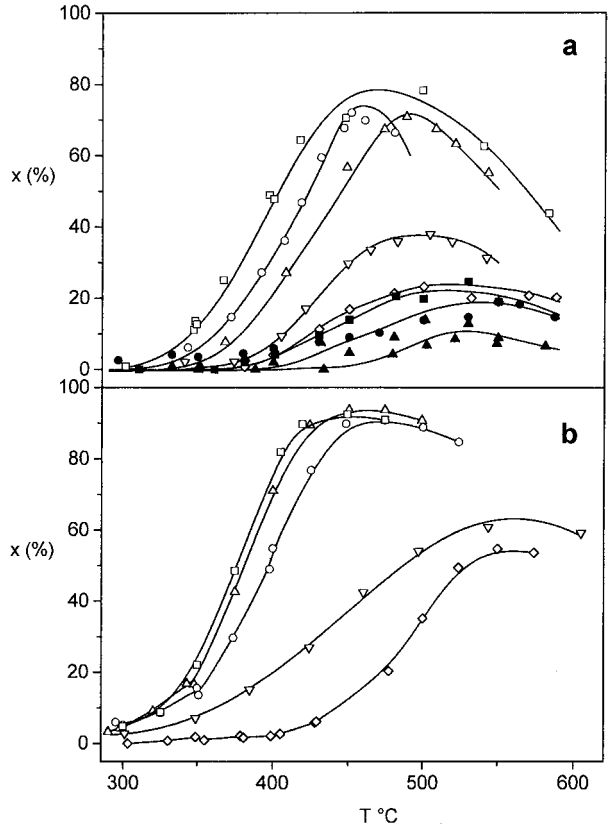

FIG. 5. Dependence of conversion of NO to N_2 in SCR of NO with CH_4 on temperature and Co/Al loading for (a) CoNaK–FER (—❐—) 0.31, (—❍—) 0.28, (—△—) 0.18, (—▽—) 0.12, (—◇—) 0.07, (—■—) 0.06, (—●—) 0.03, and (—▲—) 0.01; (b) CoH–FER (—❐—) 0.42, (—❍—) 0.25, (—△—) 0.23, (—▽—) 0.07, (—◇—) 0.05.

the conversion of NO to nitrogen is not linearly proportional to the Co content in zeolites. This implies the presence of Co ions with different activity. It is also seen that the CoH-zeolites exhibit a higher conversion than CoNa-zeolites at a similar Co concentration. This difference between CoH and CoNa forms of both zeolite structures is higher at low Co loadings than at high loadings. The effect is more pronounced with Co–ferrierites than with Co–ZSM-5.

Conversion of NO in CH_4-SCR of NO over Co_xO_y–Co–Zeolites

To elucidate the effect of dispersed cobalt oxide-like species on the SCR activity of Co-zeolites, possibly present in the highly loaded zeolites, such cobalt species were prepared in CoNa–ferrierite by transformation of a part of the exchanged Co ions into Co_xO_y species (see Table 2). The Co_xO_y–Co–FER exhibited much higher conversion of NO to NO_2 compared to CoNa–FER, but its CH_4-SCR activity in NO conversion to nitrogen was not different (see Fig. 6).

TABLE 2

Concentrations of the Individual Co Ions and Co Ions in Co_xO_y–Co–FER and in "Parent" CoNa–FER/0.12

Zeolite	Co(α)/Al	Co(β)/Al	Co(γ)/Al	Co/Al	Co(Co_xO_y)/Al
CoNaK–FER/0.12	0.02	0.09	0.01	0.12	—
Co_xO_y–Co–FER/0.12	0.02	0.06	0.01	0.1	0.03

Conversion of NO in CH_4-SCR over Co-Zeolites of MFI, FER, and MOR Topologies

Figure 7 compares conversion of NO to nitrogen depending on the temperature for Co-zeolites of different topologies at low and high concentrations of the Co ions. At low Co loadings, Co–MFI exhibited convincingly a higher activity than Co–FER. The lowest activity was found with Co–MOR. It is to be noted that the conversion values of the low Co-loaded zeolites were not affected by protonic sites, as these were not present in the CoNa-zeolites. At high Co loadings of about Co/Al 0.4, i.e., the highest loading which can be achieved for these exchanged Co-zeolites, the activity of Co–FER and Co–MFI was comparable, but that of Co–MOR was substantially lower. Moreover, low activity of Co–MOR in CH_4-SCR of NO above 500°C was also manifested in ca. 30% selectivity to CO, in contrast to Co–FER and Co–MFI, where the exclusive formation of CO_2 was observed. However, as ferrierite possessed a lower Si/Al framework ratio, and thus a higher weight content of cobalt than Co–MFI (see Table 1 and Fig. 7), it followed that the Co ions in the MFI structure, even at high loadings, exhibited the highest activity like that at the low cobalt concentration. Thus, the CH_4-SCR activity of the Co ions

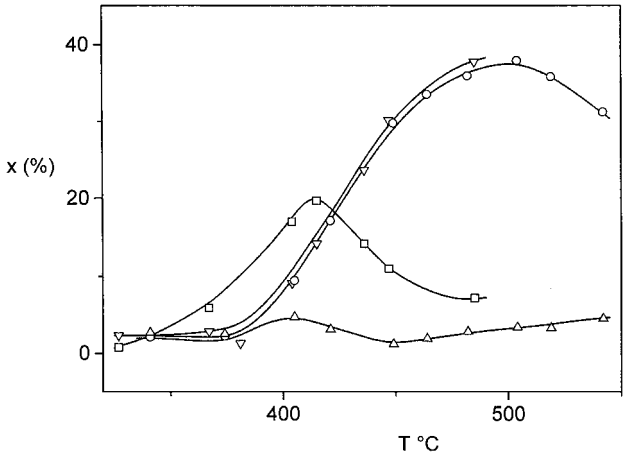

FIG. 6. Dependence of conversion of NO to (—❍—) and (—▽—) N_2 and to (—△—) and (—❐—) NO_2 in SCR of NO with CH_4 on temperature for CoNaK–FER/0.12 and Co_xO_y–Co–FER/0.12 respectively.

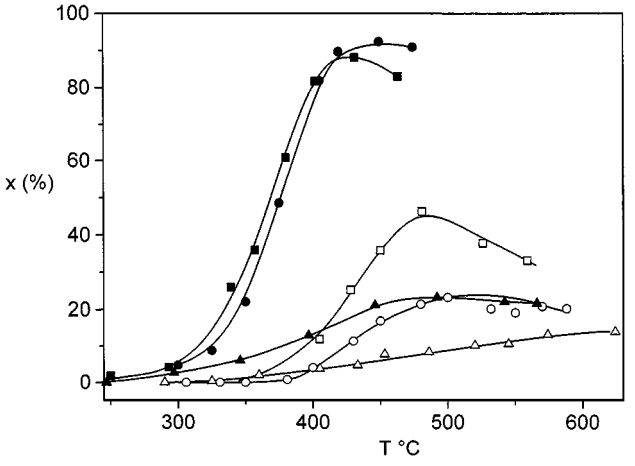

FIG. 7. Dependence of conversion of NO to N_2 in SCR of NO with CH_4 for (—❐—) CoNa–MFI/0.10, (—❍—) CoNaK–FER/0.12, and (—△—) CoBa–MOR/0.10 and (—■—) CoH–MFI/0.42, (—●—) CoH–FER/0.42, and (—▲—) CoH–MOR /0.35.

is very different, depending on the topology of the zeolite matrix.

Conversion of CH_4 over H–, CoH–, and CoNa–Zeolites

Methane oxidation by oxygen on H–ZSM-5 proceeded at temperatures above 500°C with incomplete oxidation and roughly 30% of methane was oxidized only to carbon monoxide. Both the CoNa– and CoH–zeolites exhibited much higher activity, resulting also in oxidation of methane to carbon dioxide, and the conversion did not depend on whether the Co-zeolites originated from the parent Na- or NH_4-zeolites (Fig. 8). Surprisingly, the activity of Co–ZSM-5 was much higher than that of Co–ferrierite, although the concentration of Co ions in the latter zeolite was higher than that in the former (see Table 1).

Turnover Frequency (TOF) Values of the CH_4-SCR over Co Ions in Zeolites

To compare the activity of the individual Co ions in CH_4-SCR of NO to nitrogen, it was necessary to choose a temperature at which the conversion value is below ca. 20% and below the inflection point of the conversion vs temperature profile, where the Arrhenius rate equation can be assumed to be satisfied. As this can hardly be done for the entire Co concentration range in the zeolite, we transformed the dependence of NO conversion vs temperature into an Arrhenius plot, log x_{N_2} vs $1/T$. We used the value of x_{N_2} obtained from the linear part of this dependence to calculate the reaction rates and related TOF values. This is illustrated for CoNa–FER/0.28 in Fig. 9. In cases where the conversion values were out of the limit given above for the given temperature, the extrapolated conversion values taken from a dashed line in Fig. 9 were used.

The obtained TOF values are plotted against Co/Al ratios for CoNaK–, CoH–FER and CoNa–, CoH–MFI zeolites in Figs. 10 and 11, respectively. It is seen that the TOF values do not exhibit a constant value, but depend on the Co/Al concentration. These dependences are different for CoH and CoNa forms of zeolites and also for FER and MFI structures. This observation clearly evidenced that the Co ions in the studied zeolites exhibit quite different activities, with respect not only to different zeolite structures but also to the Co ions present in one zeolite type.

To analyze the activity of the individual Co ions at different cationic sites (α, β, and γ), we used the previously determined distribution of the individual α-, β-, and γ-type Co ions in Co–ZSM-5 and Co–ferrierite samples (see

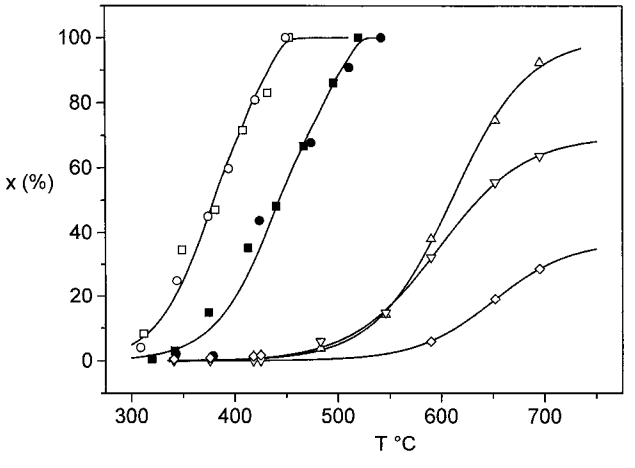

FIG. 8. Dependence of conversion of CH_4 oxidation by oxygen to CO_2 on temperature for (—❐—) CoH–MFI/0.46, (—❍—) CoNaK–MFI/0.41, (—■—) CoH–FER/0.42, and (—●—) CoNaK–FER/0.31 and for H–MFI (—△—) conversion of CH_4 to (—▽—) CO_2 and (—◇—) CO.

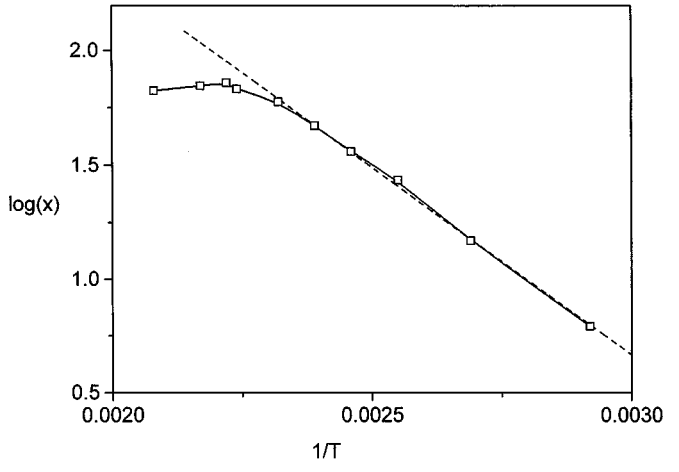

FIG. 9. Arrhenius plot of dependence of conversion of NO to N_2, $\log(x_{N_2})$ on $1/T$, over (—❐—) CoNa–FER/0.28 and (- - - -) its linear approximation.

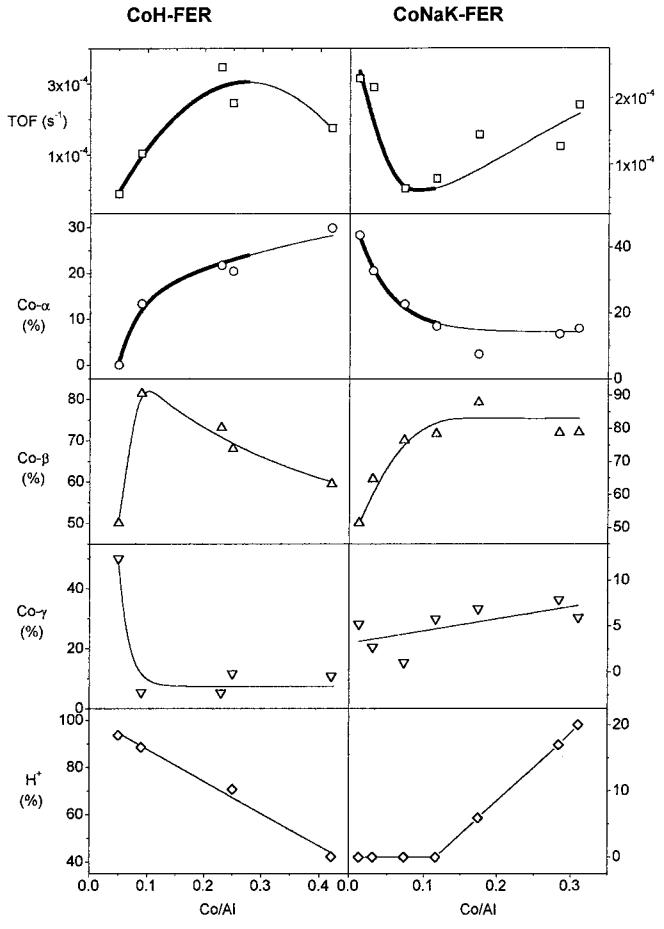

FIG. 10. Dependence of TOF, relative concentration of the α-, β-, and γ-type Co ions and relative concentration of H^+ ions to the total number of exchangeable sites, on Co/Al in CoH–FER (TOF at 400°C) and CoNaK–FER (TOF at 400°C). Bold lines indicate region taken for evaluation of this dependence.

Refs. (13) and (12), respectively); for additional samples the Co(II) Vis spectra (not shown in the figure) were monitored and analyzed according to the procedures described in Refs. (12) and (13). The concentration of protons in Co-zeolites was determined from the quantitative analysis of the IR bands at 3610 and 3604 cm^{-1}, corresponding to the bridging SiOHAl groups in ZSM-5 and ferrierite, respectively, and using extinction coefficients given elsewhere (21). With increasing Co ion exchange degree, the concentration of protons in CoH–zeolites decreased. In CoNa-zeolites at higher Co loadings, the protons, as well as the Co ions, were also exchanged (see Figs. 10 and 11).

Figures 10 and 11 relate the TOF values in CH_4-SCR of NO to nitrogen for CoH- and CoNa-zeolites of FER and MFI structures, the relative concentrations of the α-, β-, and γ-type Co ions, and the concentration of the protonic sites (relative to the total number of exchangeable sites) to the cobalt concentration (Co/Al) in zeolites. The population of the α, β, and γ cationic sites by the Co ions with increasing Co loading strongly depends on the type of co-cation (H^+ vs Na^+) present in the zeolite and on the zeolite structure. This is discussed in detail elsewhere (12, 13) where the determination of the individual α, β, and γ Co ion cationic sites in FER and MFI structures and their population by the Co ions was done.

With Co–ferrierites, the TOF value increases with increasing Co concentration, but at Co/Al above 0.3 the presence of some Co_xO_y species can be a reason for decreasing TOF values. The same trend as that of TOF vs Co/Al exhibits the relative concentration of the α-type Co ions. For CoNaK–FER the decreasing TOF values with increasing Co/Al are also in agreement with the decreasing concentration of the α-type Co ions. At Co/Al above 0.15, when, besides the Co ions, protons were also exchanged into ferrierite, their presence might be a reason for an apparent increase in the activity of the Co ions. Therefore, for a comparison of TOF values and relative concentrations of the

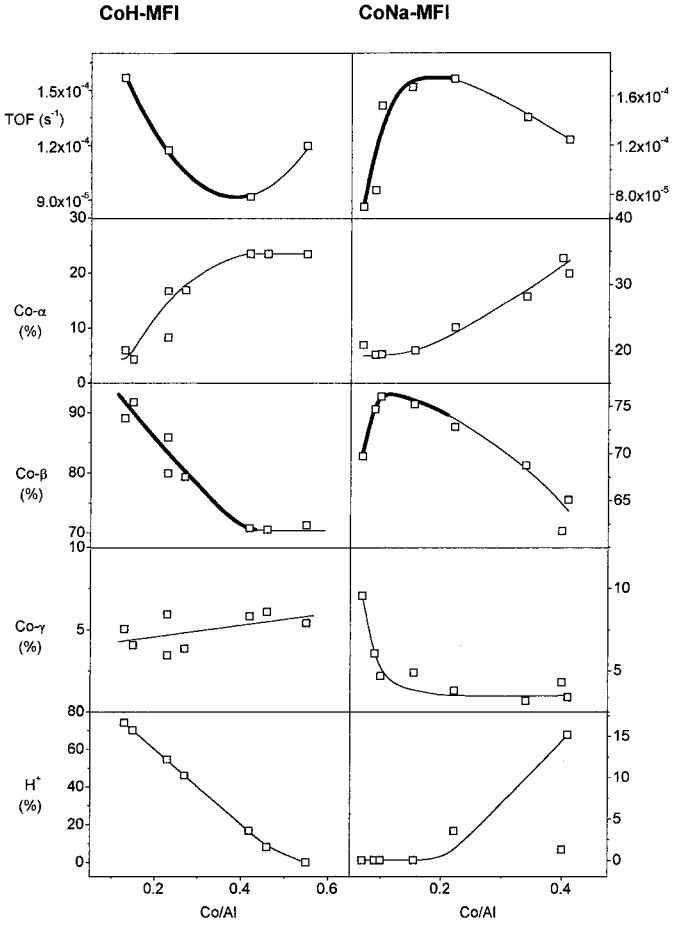

FIG. 11. Dependence of TOF, relative concentration of the α-, β-, and γ-type Co ions and relative concentration of H^+ ions to the total number of exchangeable sites, on Co/Al in CoH–MFI (TOF at 350°C) and CoNa–MFI (TOF at 370°C). Bold lines indicate region taken for evaluation of this dependence.

TABLE 3

Turnover Frequency (TOF) in CH_4-SCR of NO and Concentration of the α- and β-Type Co Ions in CoK–MOR/0.06 and CoBa–MOR/0.10; Conversion of NO at 538°C at Conditions of the Catalytic Test

Co/Al	Co (wt%)	x_{N_2} (%)	TOF (s^{-1})	α (%)	β (%)	γ (%)
0.06	0.50	3.60	6.7×10^{-5}	25	60	15
0.10	0.87	10.90	11.6×10^{-5}	60	40	

Note. Calculated TOF (α) $= 17.9 \times 10^{-5}$ and TOF (β) $= 2.1 \times 10^{-5}$ s^{-1}. Low concentration of the γ-type Co ions is not included in the calculation.

α-, β-, and γ-type Co ions depending on the total Co concentration, the zeolites with low concentrations of Co ions, where the presence of Co_xO_y species was excluded and trends of TOF values on Co/Al were not substantially affected by too high differences in the concentration of protons, were selected.

An analogous analysis, under the same conditions, was done for Co–MFI zeolites. Again, a different dependence of TOF values, as well as a different distribution of Co ions among α, β-, and γ-sites on Co/Al concentration, was obtained for CoNa– and CoH–MFI zeolites. In contrast to Co–FER, with both the CoH– and CoNa–MFI zeolites the same trend in the dependence of TOF values on cobalt concentration was obtained for the concentration of the β-type Co ions.

Table 3 provides TOF values for CH_4-SCR of NO on Co–mordenites with different concentrations of the individual Co ion types, determined elsewhere (11). In comparison with the Co–FER and Co–MFI zeolites, Co–MOR catalyzes the CH_4-SCR of NO at much higher temperatures (see Fig. 7), indicating its general lower activity. Also, oxidation of ca. 30% of methane to CO reflects low activity of the Co ions in mordenite. By comparison of the TOF values for Co–MOR (because of low activity of Co–MOR, at 538°C) with different distributions of the α- and β-type Co ions (low concentration of the γ-type cations is neglected), it follows that the α-type Co ions exhibit roughly 10 times higher activity than the β types.

DISCUSSION

It is generally accepted that the SCR of NO with methane, and paraffins generally, takes place via oxidation of NO to NO_2, followed by NO_x reduction by paraffins to nitrogen (3–5, 18, 19). Protonic sites of H–MFI, H–FER, and H–MOR oxidize NO to NO_2 (shown for H–MFI in Fig. 1), but their activity in SCR is substantially lower compared to that of Co–zeolites. This is also manifested in methane incomplete oxidation to a mixture of carbon monoxide and dioxide. The activity of H-zeolites in CH_4-SCR of NO follows the sequence H–MFI $\gg$ H–FER > H–MOR, although H–FER and H–MOR contain many more protonic sites (1.70 compared to 1.05 mmol/g for H–MFI). This sequence is analogous to that one found for CH_4-SCR of NO and methane oxidation with Co-zeolites, showing the strong influence of zeolite structure on zeolite activity, even though factors other than zeolite topology may be involved.

Contribution of protonic sites to the SCR activity of CoH-zeolites is obvious, as it follows from a comparison of the activity of Co-zeolites given in parts (a) and (b) of Figs. 4 and 5 and in Figs. 10 and 11. For both MFI and FER zeolite structures, the activity of CoH-zeolites is higher compared to that of CoNa forms. As the SCR activity of protons is very low, it implies that they contribute to this reaction mostly via enhancement of the rate of oxidation of NO to NO_2. A similar function might be ascribed to cobalt oxide-like species present, besides the Co ions, in highly loaded zeolites. As shown in Fig. 6, the presence of cobalt oxide-like species in the zeolite increases substantially NO conversion to NO_2 at a lower temperature and thus the rate of NO_2 formation. This can be expected to enhance the rate of SCR of NO, the result of which is the same NO conversion for the zeolite containing a lower concentration of the exchanged Co ions and some Co_xO_y species. An increase in the rate of the SCR reaction for Co-zeolites containing, in addition to the Co ions, dispersed cobalt oxide species was also reported by Stakheev *et al.* (20). To summarize, both the protonic sites and cobalt-oxide-like species contribute to CH_4-SCR of NO by enhancement of the rate of NO_2 formation; however, their own activity in the SCR reaction is low.

To understand the different activities of the Co zeolites with different topologies, we have attempted to analyze the activity of the individual Co ions in zeolites of MFI, FER, and MOR structures. This has been enabled by knowledge of the distribution of the exchanged Co ions among the individual cationic sites in zeolites, as obtained from quantitative analysis of the characteristic Vis spectra of the Co(II) ions. It was evidenced that the ion-exchanged Co-zeolites up to the concentration of Co/Al 0.35, used in this study, did not contain cobalt oxide species, which might be possibly formed by hydrolysis of cobalt salt solutions during ion exchange. The presence of exclusively exchanged Co ions in low Co-loaded zeolites follows from the quantitative analysis of the IR bands of antisymmetric T–O–T vibrations in the region of skeletal vibrations induced by the Co ions situated exclusively at the cationic sites (see Refs. (14) and (15). Therefore, the reported TOF values for Co zeolites with the cobalt concentration below Co/Al $= 0.35$ reflect the activity of the exchanged Co ions. As already pointed out, prevailing importance in the analysis of the activity of the individual Co ions has been given to the results obtained with Co-zeolites containing non-transition-metal ions and not protons as co-cations.

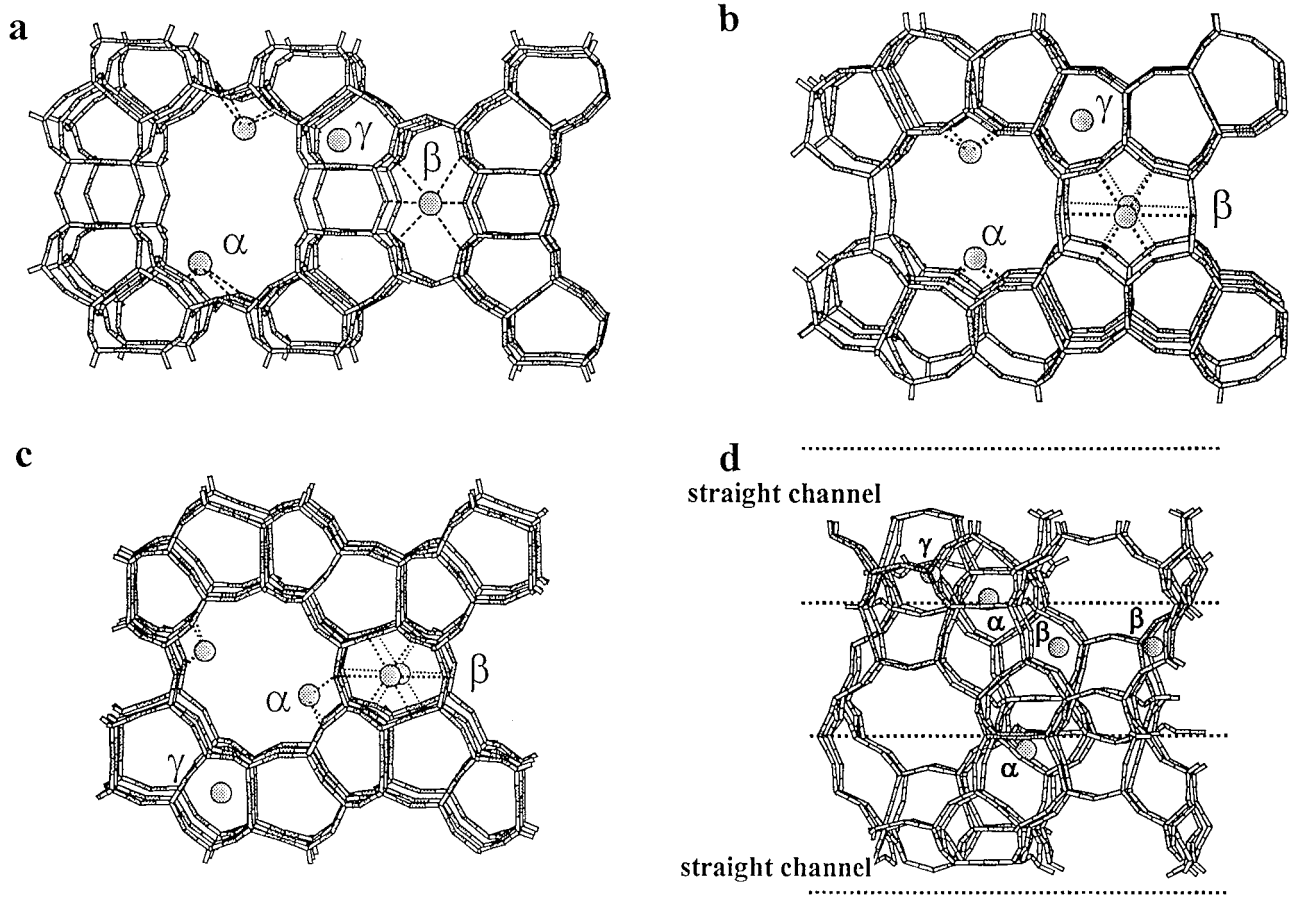

FIG. 12. Suggested cationic sites of the α-, β-, and γ-type Co ions in (a) MOR, (b) FER, and (c) and (d) MFI structures (cf. Refs. 11–13, respectively); (c) view through the straight channel and (d) view through the sinusoidal channel, straight channel indicated by dashed lines.

Figures 12 and 13 illustrate the location of the α-, β-, and γ-type Co ions in MFI, FER, and MOR frameworks as analyzed and suggested elsewhere (see Refs. (13), (12), and (11), respectively):

(i) The α-type Co ions are coordinated to the walls of the main channel of mordenite (site E according to the notation of Mortier, cf. Ref. (10)) and ferrierite (site B) and the straight channel of the ZSM-5 structure. They are suggested to be coordinated to framework oxygens of six-member rings formed from two-folded pentasil rings. The α-type Co ions exhibit the weakest bonding to framework oxygens among the Co ions.

(ii) The β-type Co ions are suggested to be coordinated to framework oxygens of the twisted eight-member rings of the mordenite cavity (site A), of the deformed six-member rings of the ferrierite cavity (site G), and of the deformed six-member rings at the intersection of the straight and sinusoidal channels of the ZSM-5 structure. Perturbation of the framework bonds at the β cationic sites by these Co ions indicates medium strength of bonding to framework oxygens.

(iii) The γ-type Co ions are in the so-called "boat-shaped" site of mordenite (site C, see Ref. (10)) and analogous framework local structures in ferrierite and ZSM-5. This Co site represents the most packed highly coordinated Co ion with the highest strength of Co ion bonding to framework oxygens.

It is to be pointed out that the population of the individual sites by the Co ions depends on the concentration of cobalt in the zeolite, on the presence of co-cations, namely, protons or non-transition-metal ions, and on the zeolite structural type. With all the zeolite structures studied here, the most populated site is the β site (50%–70%), followed by the α site (10%–30%), and then by the least populated γ site (0%–15%). Therefore, to simplify the analysis of different activities of Co-zeolites of MFI, FER, and MOR structures, we have focused on the activity of the cobalt α and β sites. It should also be mentioned that all the Co ions in MFI, FER, and MOR zeolites are accessible to all reactants and products of the CH_4-SCR reaction.

From the analysis of the dependence of TOF values and relative concentrations of the α-, β-, and γ-type Co ions on

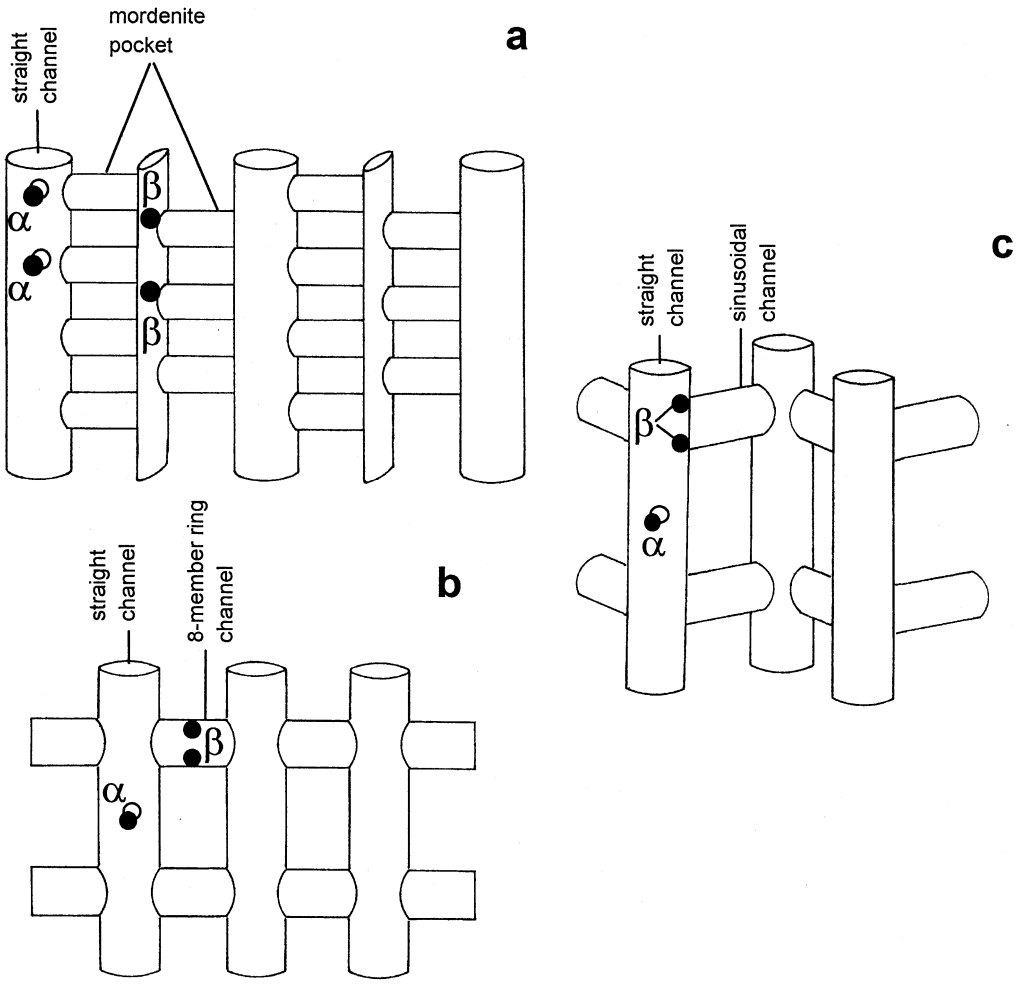

FIG. 13. Schematic representation of cationic sites in the channels of (a) mordenite, (b) ferrierite, and (c) ZSM-5.

cobalt content in ferrierite and ZSM-5 (Figs. 10 and 11) and the TOF values for the α- and β-type Co ions in mordenite (Table 3, see also Figs. 12 and 13), it follows:

(i) In ferrierite and mordenite, the most active sites are suggested to be the α-type Co ions. These ions are coordinated to framework oxygens in the main channel of mordenite and the main ten-member ring channel of ferrierite. The highly active α-type Co ions are easily accessible to reactants and intermediates and they exhibit the weakest bonding to framework oxygens among the individual Co ions (cf. Refs. (3), (11), (12), and (15));

(ii) On the other hand, in ZSM-5, surprisingly, the β-type Co ions are indicated to be the most active sites. These Co sites are coordinated to oxygens in the deformed six-member ring of the MFI structure (cf. Ref. (13)) like in ferrierite. But the β site in the MFI structure is located just at the intersection of the straight and sinusoidal channels, in contrast to the β sites in ferrierite and mordenite, where it is in the eight-member ring and the interconnecting channel, respectively. This observation points out that for the activity of the Co ions in CH_4-SCR of NO not only the expected strength of bonding of the Co ions to the framework but also cation location in the inner volume of the zeolite might be important, although all the Co ions are accessible to reactants.

This implies that the β-type Co ions in the MFI structure are located at the most advantageous position with respect to the reactant adsorption and formation of reaction intermediates. With MOR and FER structures, the β-type Co ions are also accessible to the CH_4-SCR reactants, but as they are located in the interconnected small channel of mordenite and inside the small eight-member ring channel of ferrierite, they might be diffusionally hindered compared to the α-type Co ions located in the main channels of ferrierite and mordenite and compared to the β-type Co ions in the MFI structure.

However, there might also be another factor affecting the rate of the catalytic reaction, i.e., distances of the Co ions, if the SCR reaction proceeds with the participation of the two neighboring sites. It can be assumed that, at one

site, oxidation of NO to NO_2 takes place, and the other site is involved in the activation of methane. The active sites might be two Co ions, a Co ion with a proton, or a Co ion with a Co_xO_y species. While the distances between the Co ions, and protons or Co_xO_y species cannot be estimated, a rough estimation of distances was done for the exchanged Co ions between the most populated Co ion sites, i.e., the α- and β-type Co ions in MOR, FER, and MFI structures. The distances were calculated from the XRD data of the "naked" MOR, FER, and MFI frameworks and under the following geometrical simplifications. The α-type Co ions are located in the plane of the rectangle of the six-member ring, forming the wall of the main channel of mordenite and the straight ten-member ring channel of ZSM-5 and ferrierite, and the β-type Co ions are placed in the center of the twisted eight-member ring of mordenite and in the center of the deformed six-member ring of ferrierite and ZSM-5. The closest Co sites have been found with the β-type Co ions in the MFI structure (ca. 4.7 Å), while in ferrierite the closest sites are represented by the α-type Co ions (ca. 5.6 Å). The distances between the other Co sites are much greater. Therefore, it can be suggested that the distances between the Co active sites, differing substantially in the individual studied zeolites, might also contribute to the different activities of the individual Co ions and thus to the activities of Co-zeolites with different topologies.

CONCLUSIONS

From the simultaneous analysis of the distribution of Co ions at three cationic sites, denoted as α, β, and γ, of the presence of protons or sodium as co-cations, and of cobalt oxide-like species in Co–ZSM-5, Co–ferrierite, and Co–mordenite, and their conversion in SCR of NO with methane, the following conclusions can be made:

(i) Protons and cobalt oxide-like species contribute to the CH_4-SCR reaction, by enhancement of the rate of oxidation of NO to NO_2.

(ii) The effect of zeolite topology on the CH_4-SCR catalytic activity of the Co ions in zeolites is dramatic. The highest activity, in terms of TOF values per average Co ion, shows the Co ions in ZSM-5 followed by those ions in ferrierite and with those ions in mordenite showing the lowest activity. However, as Co–ferrierite (Si/Al 8.4) can accommodate more Co ions, the activity of Co–ZSM-5 (Si/Al 12.5) and Co–ferrierite with complete Co loading per unit weight of the Co–zeolite are comparable. Thus, generally, because of the possible synthesis of the ferrierite framework with Si/Al of ca. 8 compared to ZSM-5 with a minimum Si/Al of ca. 12, their reaction rates per unit weight of the catalyst in the CH_4-SCR of NO are comparable.

(iii) The individual α-, β-, and γ-type Co ions in all the studied zeolites (see Fig. 12) are accessible to the reactants and might also be accessible to the expected intermediates of the CH_4-SCR reaction, but their catalytic activity is quite different. This finding originates from their coordination at different cationic sites with different strengths of Co ion bonding to framework oxygens and different positions of the exchanged cations in the inner volume of the zeolite, given by its topology.

(iv) The most active Co sites in ferrierite and mordenite are suggested to be the α-type Co ions. These ions are coordinated to framework oxygens in the wall of the main channel of mordenite and the main ten-membered ring channel of ferrierite. They are easily accessible to reactants and intermediates and exhibit the weakest bonding to framework oxygens among the Co ions. The most populated β-type Co ions in ferrierite and mordenite, located in the eight-member ring channels and interconnected narrow channels, respectively, might be diffusionally hindered. In addition, smaller Co–Co distances for the α-type Co ions in ferrierite are suggested to contribute to much higher activities of Co–ferierites than at Co–mordenites.

(v) In contrast to Co–FER and Co–MOR, with Co–MFI the most populated β-type Co ions were indicated to be the most active sites. These Co sites are coordinated to oxygens in the deformed six-membered ring of the MFI structure as in ferrierite, but in contrast to ferrierite they are located at an advantageous position, at the intersection of the straight and sinusoidal channels. Moreover, the Co–Co distances between the β-type Co ions in ZSM-5 are the shortest among the three Co ion types and those ions located in different topologies. All these factors might contribute to the activity of the Co ions being highest in ZSM-5 zeolite.

It can be summarized that the combination of kinetic and spectroscopic results allowed us to identify the most active Co sites in the Co-zeolites of MFI, FER, and MOR structures in CH_4-SCR of NO and thus to explain the different activities of the Co-zeolites with different topologies. This showed that the location of the Co ions in the inner zeolite volume, their coordination, and the distances between the Co ions play important roles in their catalytic activity in the CH_4-SCR of NO. But the degree of contribution of these individual factors to the resulting activity of the Co ions is still not clear and requires further study. The siting of the Co ions in the zeolite structure, highly important for their activity, is governed, besides the distribution of aluminium in the framework, by the zeolite topology providing local framework structures, which satisfy requirements of the Co ions for their coordination.

ACKNOWLEDGMENTS

The authors acknowledge financial support of the Academy of Sciences of the Czech Republic under Project S4040016 and from the Air Products and Chemicals, Inc., Pennsylvania.

REFERENCES

1. Iwamoto, M., and Yahiro, H., *Catal. Today* **22**, 5 (1994).
2. Shelef, M., *Chem. Rev.* **95**, 209 (1995).
3. Wichterlová, B., Dědeček, J., and Sobalík, Z., *in* "Proceedings 12th International Zeolite Conference, 1998" (M. M. J. Treacy, B. K. Marcus, M. E. Bisher, and J. B. Higgins, Eds.), p. 941. Materials Research Society, Warrendale, PA, 1999.
4. Li, Y. J., and Armor, J. N., *J. Catal.* **150**, 376 (1994).
5. Li, Y. J., Slager, T. L., and Armor, J. N., *J. Catal.* **150**, 388 (1994).
6. Li, Y. J., and Armor, J. N., *Appl. Catal. B* **5**, L257 (1995).
7. Li, Y. J., and Armor, J. N., *J. Catal.* **145**, 1 (1994).
8. Armor, J. N., *Catal. Today* **26**, 147 (1995).
9. Yogo, K., Ihara, M., Terasaki, I., and Kikuchi, E., *Catal. Lett.* **17**, 303 (1993).
10. Mortier, W. J., *in* "Compilation of Extraframework Sites in Zeolites." Butterworth, London, 1982.
11. Dědeček, J., and Wichterlová, B., *J. Phys. Chem. B* **103**, 1462 (1999).
12. Kaucký, D., Dědeček, J., and Wichterlová, B., *Microporous Mesoporous Mater.* **31**, 75 (1999).
13. Dědeček, J., Kaucký, D., and Wichterlová, B., *Microporous Mesoporous Mater.* **35–36**, 483 (2000).
14. Sobalík, Z., Tvarůžková, Z., and Wichterlová, B., *J. Phys. Chem. B* **102**, 1077 (1998).
15. Sobalík, Z., Dědeček, J., Ikonnikov, I., and Wichterlová, B., *Microporous Mesoporous Mater.* **21**, 525 (1998).
16. Sobalík, Z., Dědeček, J., Kaucký, D., Wichterlová, B., Drozdová, L., and Prins, R., *J. Catal.* **194**, 330 (2000).
17. Kaucký, D., Dědeček, J., Vondrová, A., Sobalík, Z., and Wichterlová, B., *Collect. Czech. Chem. Commun.* **63**, 1781 (1998).
18. Ogura, M., Aratani, N., and Kikuchi, E., *in* "Progress in Zeolite Microporous Materials" (H. Chon, S.-K. Ihm, and Y. S. Uh, Eds.), Elsevier, Amsterdam 1997. *Stud. Surf. Sci. Catal.* **105**, 1593 (1997).
19. Lobree, L. J., Aylor, A. W., Reimer, J. A., and Bell, A. T., *in* "Proceedings, 11th International Congress on Catalysis, Baltimore, 1996 (J. W. Hightower, W. N. Delgass, E. Iglesia, and A. T. Bell, Eds.). Elsevier, Amsterdam, 1996. *Stud. Surf. Sci. Catal.* **101**, 661 (1996).
20. Stakheev, A. Y., Lee, C. W., Park, S. J., and Chong, P. J., *Catal. Lett.* **38**, 271 (1996).
21. Wichterlová, B., Tvarůžková, Z., Sobalík, Z., and Sarv, P., *Microporous Mesoporous Mater.* **24**, 223 (1998).